Available online at www.sciencedirect.com
ScienceDirect
Journal of the European Ceramic Society 30 (2010) 705–712
www.elsevier.com/locate/jeurceramsoc

Fracture resistance of a doped PZT ceramic for multilayer piezoelectric actuators: Effect of mechanical load and temperature

Raul Bermejo [a,*], Hannes Grünbichler [a,b], Josef Kreith [a,b], Christoph Auer [c]

[a] *Institut für Struktur- und Funktionskeramik, Peter-Tunner-Straße 5, Montanuniversität Leoben, 8700 Leoben, Austria*
[b] *Materials Center Leoben Forschung GmbH, Roseggerstraße 12, 8700 Leoben, Austria*
[c] *EPCOS OHG, Siemensstraße 43, 8530 Deutschlandsberg, Austria*

Received 8 April 2009; received in revised form 11 August 2009; accepted 13 August 2009
Available online 23 September 2009

Abstract

The fracture resistance behaviour of a doped lead zirconate titanate (PZT) ceramic after combined thermo-mechanical loading is investigated between room temperature (RT) and 400 °C, *i.e.* above the Curie temperature (T_C). The thermal- and stress-induced depolarisation effects due to domain switching have been assessed by the indentation method on bulk PZTs. This has been extended to multilayered actuators. Experimental findings show a depolarisation effect with the temperature, which is significantly enhanced when combined with mechanical loading. This partial or even full depolarisation of the PZT material below T_C leads to important anisotropy effects in the fracture resistance of the piezo-ceramic, which should be taking into account in the design of multilayer actuators where the direction of crack propagation (*i.e.* parallel or normal to electrodes) can affect the actuator functionality.

Keywords: PZT; Actuators; Thermo-mechanical compression test; Fracture; Toughness and toughening

1. Introduction

The outstanding piezoelectrical properties of lead zirconate titanate (PZT)-based ceramics are widely employed in the fabrication of actuators used in applications that require precision displacement control or high generative forces, *i.e.* precision mechano-electronic and semiconductor devices. In particular, multilayer piezoelectric actuators, referred to as MPAs, are currently used to control modern fuel injection systems.[1,2] MPAs are designed as a stack of thin piezo-ceramic layers which are separated by very finely printed metallic electrodes. Due to this design high electric fields and large elongations can be reached with relatively low voltages.[3] The corresponding strains are of the order of 0.1% (for a typical stack length of about 40 mm the elongation is approximately 40 μm). This elongation can be attained in a very short time (in the order of milliseconds), allowing for fast and accurate flow of fuel into the combustion chamber. The effectiveness of such an injection process (low fuel consumption, reduction of emissions) is based on the reliable functionality of the MPA over its lifetime, *i.e.* order of 10^9 cycles. In this regard, the relatively large displacements and large forces within the MPA along with the combined thermal, electrical and mechanical loadings yield nonlinear effects, which may lead to degradation of the performance of the MPA.[4,5] In service, for instance, the actuating-process is indeed a result of the periodic reorientation (domain switching) of the piezoelectric crystals in the PZT in the ferroelectric phase, *i.e.* below the Curie temperature. During this process, cyclic inelastic deformation and Joule heating occur. These effects may lead to periodic tensile stresses concentrated around the electrode-tips, which can induce fatigue damage (the growth of cracks) in the ceramic material, thus affecting the structural and functional integrity of the MPA.[6] In addition, although these MPAs operate under externally applied compressive stresses, failure of components in service has been reported associated with the propagation of cracks within the electrode–ceramic multilayered structure.[7] Therefore, to ensure such high reliability of the ceramic components uncontrolled propagation of cracks must be avoided completely.

The investigation of the initiation and subsequent growth of cracks in piezo-ceramic materials is of primary importance

* Corresponding author. Tel.: +43 3842 402 4115; fax: +43 3842 402 4102.
E-mail address: raul.bermejo@unileoben.ac.at (R. Bermejo).

0955-2219/$ – see front matter © 2009 Elsevier Ltd. All rights reserved.
doi:10.1016/j.jeurceramsoc.2009.08.013

and has been the focus of many researchers. A review of experimental results to interpret the essential features of crack growth in ferroelectric ceramics can be found in Ref. [8]. Considerable work has been done to analyse the behaviour of monolithic piezo-ceramics to determine the crack growth resistance (R-curve) with respect to defined electrical boundary conditions.[4,9–18] In fuel injection applications, however, a combination of electrical, mechanical and thermal loads is applied to the ceramic device. The complex architecture of MPAs leads to additional residual stresses resulting from sintering and poling processes involved in fabrication. The combination of electrical, thermal and mechanical loads, acting in critical regions of the MPA, may yield a different fracture resistance when applied in service compared to that exhibited by bulk ceramics and, thus, should be also analysed.

The motivation of this work is to assess the fracture resistance of a doped PZT piezo-ceramic material as a function of applied thermo-mechanical loads between room temperature and 400 °C, *i.e.* above the Curie temperature. This aims to simulate, to some extent, the real thermo-mechanical fracture behaviour of the PZT ceramic material used in MPAs during service. For such purpose, the indentation fracture (IF) method (a feasible method to evaluate small volumes like available in multilayer actuators) is employed to estimate the fracture resistance of a doped PZT ceramic as a function of loading conditions. The depolarisation effects associated with thermal-induced switching processes are investigated on poled specimens after exposure at different temperatures. Non-poled specimens are also used as a reference material. Additionally, mechanical loads are applied in compression at different temperatures to determine the influence of the combined thermo-mechanical loading on the depolarisation of PZTs. The indentation crack lengths are measured before and after the tests to account for the fracture resistance anisotropy of the piezo-ceramic material, which depends on the remnant poled state of the specimens after testing. Finally, a multilayered actuator is investigated in order to assess the fracture resistance of the piezo-ceramic in the different regions (active and passive) after the application of mechanical (compressive) loads.

2. Experimental

2.1. Materials of study

2.1.1. Bulk material

A commercial soft doped PZT ceramic with a composition near the morphotropic phase boundary (with a Curie temperature of ≈340 °C) has been used in these experiments. The material was designed as a stack of thin piezo-ceramic layers sintered at approx. 1100 °C in a lead-enriched atmosphere. The sintered plates were ground to the finished shape and rectangular section bar specimens of dimensions 4 mm × 3 mm × 10 mm were cut from the plate. Cr–Ag-electrodes were then deposited by a sputtering process onto the end surfaces for poling purposes. Two sides of the specimens were polished with diamond paste down to 1 μm for a better identification of the indentation cracks. The specimens were then poled longitudinally (along the largest dimension) with an electrical field of 2 MV/m (Fig. 1). Some specimens were kept "as-sintered", *i.e.* in the non-poled state, for comparison studies and microstructural characterisation. Density was determined using Archimedes method resulting in 7.92 g cm^{-3}. Grain size was estimated by the linear intercept method ranging between 0.5 μm and 3 μm, with a mean value of ≈1.5 μm. Fig. 2 shows a microstructure of a non-poled PZT bulk specimen after being polished and chemically etched. It can be inferred from the figure the random alignment of domains within the different grains.

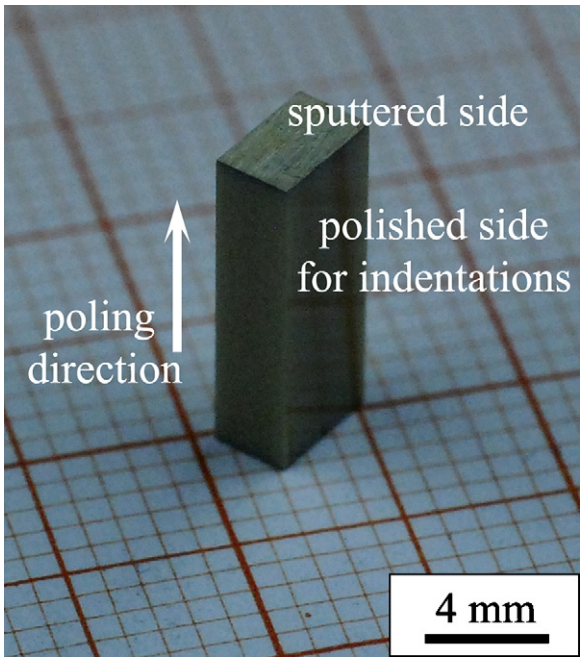

Fig. 1. Bulk PZT specimen showing the sputtered surfaces, the polished surfaces and the direction of poling.

2.1.2. Multilayered actuator

Commercial PZT-based multilayer piezoelectric actuators have been used in the experiments. They were designed as a stack of thin piezo-ceramic layers which are separated by interdigitated metallic electrodes (Fig. 3). The electrode patterns were

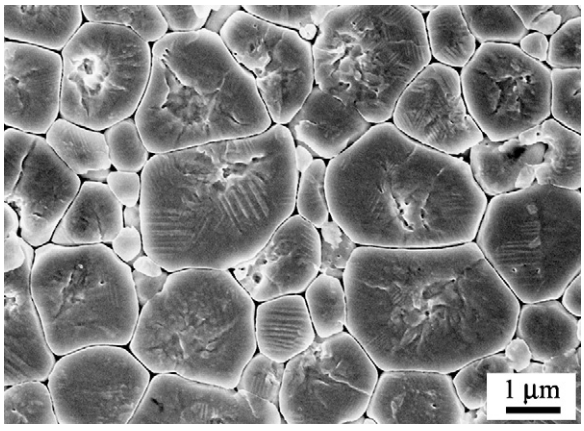

Fig. 2. SEM micrograph of the microstructure of the PZT bulk material. A random alignment of domains can be seen within the grains.

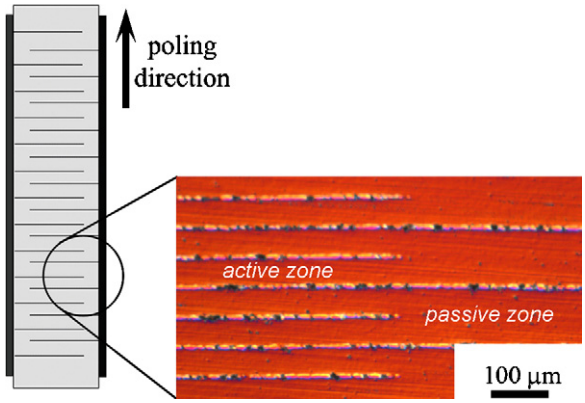

Fig. 3. Multilayer piezoelectric actuator scheme used in fuel injection systems. A detail of the active and passive zones is presented. The poling direction is normal to the electrodes.

printed with silver/palladium-paste on green sheets of the PZT ceramic. The sheets were stacked, pressed and cut into single elements (stacks). Then they were sintered under the same conditions as for the PZT bulk material. The sintered bodies were ground to the finished shape and external termination was made by firing a silver paste on the outside of the sintered stacks. All stacks were pre-stressed (*ca.* −15 MPa to −25 MPa in magnitude) and electrically poled (along the longitudinal axis) by applying an electrical field of *ca.* 2 MV/m.

2.2. Indentation fracture and thermo-mechanical tests

2.2.1. Bulk specimens

Indentation tests were performed in both poled and non-poled bulk specimens using a Vickers indenter (Zwick GmbH, Ulm, Germany) up to a maximum load of 9.8 N and holding time of 10 s. At least three indentations were placed along the polished surface of each specimen in a way that the resulting cracks were parallel or perpendicular to the direction of applied electrical field (specimen longitudinal direction), as illustrated in Fig. 4. The length of the indentation cracks were then measured with an optical microscope (Olympus Austria GmbH, Vienna, Austria), before conducting the thermo-mechanical tests, in order to have a reference crack length mean value. In order to check the accuracy in the measurement using the optical microscope some specimens were brought into SEM (Zeiss EVO 50, Germany) to allow a very clear and precise identification of the crack tip. The difference in crack length measurements for every bulk specimen was less than 5%, both with optical microscope and with SEM.

Combined thermal and mechanical loads were then applied to the specimens by means of a temperature chamber (Carbolite GmbH, Ubstadt-Weiher, Germany) coupled to an adapted universal testing machine (Messphysik Materials Testing GmbH, Fürstenfeld, Austria), which enables the measurement of mechanical stress, strains, electrical charge (polarisation) and applied voltage (electrical field strength).

The temperature tests were performed following a ramp with a heating rate of 2 °C/min and a dwell of 30 min at the aimed temperature. The selected testing temperatures were 25 °C (RT), 75 °C, 150 °C, 225 °C, 300 °C, and 400 °C. The compression tests were performed at a loading rate of 0.5 mm/min and the maximal load was maintained for 1 min. The specimen was set in the machine with the longitudinal axis (poling axis) parallel to the loading axis.

In order to investigate the pure effect of temperature on the fracture resistance of the poled specimens, the tests were first performed without mechanical stress (*i.e.* $\sigma = 0$ MPa); non-poled specimens were also tested at the same temperatures for comparison. Further, the combination of temperature and mechanical stress (compression) was assessed with individual compression tests (*i.e.* $\sigma = -25$ MPa and $\sigma = -50$ MPa) for each selected testing temperature.

After the thermo-mechanical tests, the specimens were removed from the testing set-up and new indentation cracks were introduced in the tested specimens at room temperature. The crack lengths of the new indentations were measured and compared with the initial reference values, measured before testing, as described above.

2.2.2. MPAs

The multilayered piezoelectric actuators were mechanically loaded in the longitudinal direction (*i.e.* poling direction) using a universal testing machine (Messphysik Materials Testing GmbH, Fürstenfeld, Austria) with a load cell of 10 kN. The mechanical stresses induced during compression loading was selected between $\sigma = 0$ MPa and $\sigma = -190$ MPa. Although the region of interest for MPAs (based on performance mea-

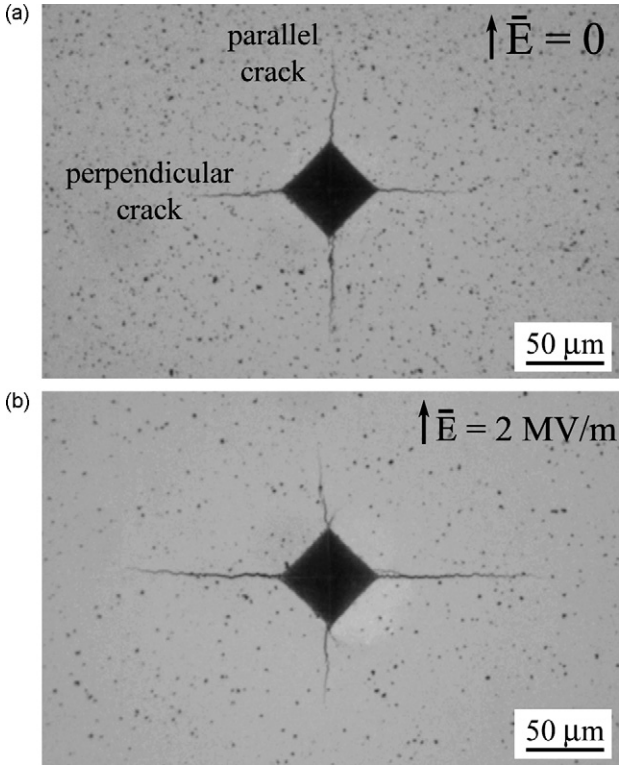

Fig. 4. Indentation cracks parallel and perpendicular to the longitudinal direction in (a) non-poled specimens, *i.e.* $E = 0$ MV/m and (b) poled specimens, *i.e.* $E = 2$ MV/m, before the thermo-mechanical tests.

surements and pre-stressed conditions) lies between −25 MPa and −50 MPa,[19] the maximum applied compression stress of −190 MPa was selected based on the fact that beyond such compressive pre-stress (so-called "blocking force") the stack will undergo no mechanical strain under service conditions (which would not make sense from the application point of view of the actuator). A second reason to reach such high compressive stresses was to ensure full depolarisation of poled stacks and thus be able to discern (if any) fracture resistance anisotropy effects within the stacks parallel and perpendicular to the poling direction.

After the tests the stacks were removed from the testing set-up for material characterisation. The specimens were ground until both regions of the stack, *i.e.* active and passive (Fig. 3), were visible, and then were polished using diamond paste suspension down to a finishing of 1 μm. The procedure was performed under low pressure to minimise any polishing effect on the microstructure of the stacks. The indentation tests were performed using a Vickers indenter (Zwick GmbH, Ulm, Germany) up to a maximum load of 1.96 N and holding time of 10 s. At least 10 indentations were placed in the middle of both active and passive zones of the stack for crack length measurements. The cracks resulting from the indentations were measured with the optical microscope to evaluate the fracture resistance of the piezo-ceramic in the different regions of the actuator as a function of the pre-stressed conditions, similar to the case of bulk material. In this case, the error in the crack length measurements was also smaller than 5%. Only in some cases, particularly in the active zone, the crack length measurement error raised up to *ca.* 10% due to the small indentation load applied.

3. Results and discussion

3.1. Evaluation of the fracture resistance

The fracture resistance was evaluated for every testing condition following the relation proposed by Anstis et al. using the IF method,[20] by measuring the length of the indentation cracks both parallel ($2c^{//}$) and normal ($2c^{\perp}$) to the longitudinal axis of the specimen:

$$K_F = \chi \cdot \frac{P}{c^{3/2}}, \tag{1}$$

where χ is a parameter related to the shape of the indentation crack, P (in N) is the indentation load and c (in m) is half the length of the measured indentation crack, as depicted in Fig. 4.

In order to estimate the χ parameter used in the IF method, the value of K_F (intrinsic to the material) should be known. Assuming an "as-sintered" state (*i.e.* non-poled) for the PZT material, five single edge V-notched beam (SEVNB) specimens were prepared for the determination of the fracture toughness (see Fig. 5) .[21] A notch radius as fine as ≈5 μm could be achieved at the notch tip. Since the mean microstructural unit of this PZT material is ≈1.5 μm, the fracture toughness value determined using the SEVNB method might be slightly overestimated.[22] However, some damage (cracks) at the notch root during notching could be observed, which indeed diminishes the influence of the notch on the fracture toughness estimation. We caution the reader that, due to the R-curve behaviour exhibited by PZTs, the fracture toughness determined through the SEVNB method will correspond to one point of the R-curve, which may not coincide with the plateau value. Nevertheless, this value will be used only as a reference value for the assessment of fracture resistance using the IF method.

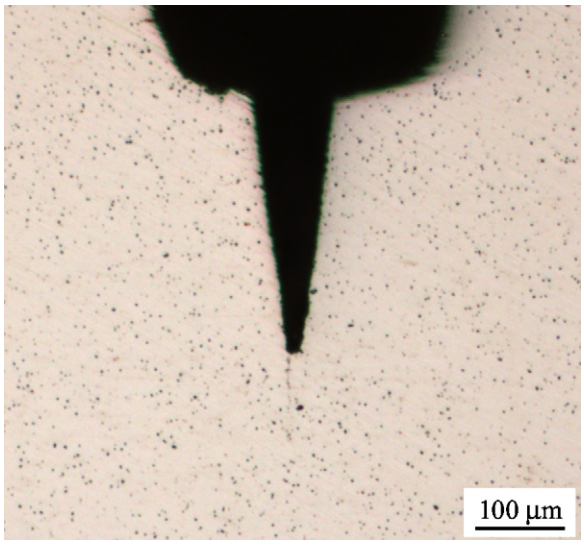

Fig. 5. Pre-notched PZT bulk specimen for fracture toughness determination.

Four point bending tests (outer and inner spans of 30 mm and 15 mm, respectively) were performed in 40 mm × 3.5 mm × 4 mm specimens following the norm standards ENV–843–1[23] and the fracture toughness was evaluated according to

$$K_{Ic} = \sigma_f \cdot Y \cdot \sqrt{a}, \tag{2}$$

where σ_f is the failure stress (in MPa), a is the crack length (in m) and Y is a geometric factor defined for an edge crack and given by[24]

$$Y = \frac{1}{(1-\alpha)^{3/2}}\left[1.9887 - 1.326\alpha - \frac{\alpha(1-\alpha)}{(1+\alpha)^2}(3.49 - 0.68\alpha + 1.35\alpha^2)\right]; \quad \alpha = \frac{a}{W} \tag{3}$$

where W (in m) is the specimen thickness. A fracture toughness value K_{Ic} of 1.09 ± 0.08 MPa m$^{1/2}$ was obtained. Taking this value as the toughness of the PZT material, the parameter χ was estimated using Eq. (1) by measuring the crack length of an indentation load of 9.8 N (*i.e.* $c \approx 100$ μm), resulting in a value of 0.11 ± 0.01. For the case of multilayered actuators, χ was also estimated using Eq. (1) by measuring the crack length following indentation at a load of 1.96 N, corresponding to the

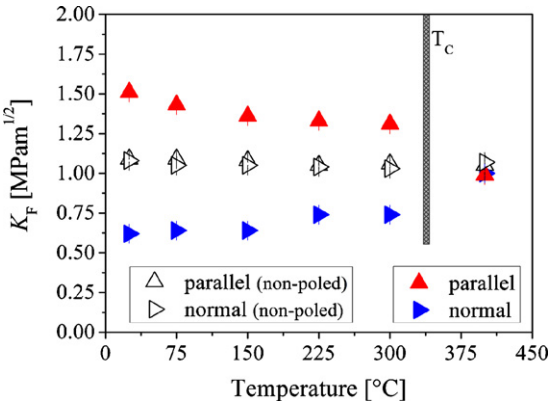

Fig. 6. Fracture resistance measured in poled and non-poled PZT specimens after exposure at different temperatures. Whereas the fracture resistance remains constant and isotropic (*i.e.* same crack length parallel and normal to the longitudinal axis) in the non-poled specimens after the testing temperatures, an effect of the temperature on K_F of the poled specimens can be appreciated, leading to partial depolarisation.

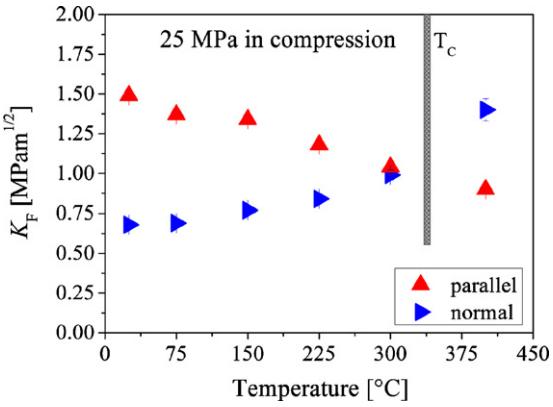

Fig. 7. Fracture resistance measured in poled PZT specimens after being mechanically stressed at $\sigma = -25$ MPa (compression) at elevated temperatures. Although a slight change in the fracture resistance (K_F) can be appreciated for exposure temperatures between 25 °C and 150 °C, the most significant change is clearly seen at 300 °C. At this temperature, K_F in parallel and normal directions is practically the same as that of the non-poled specimens. Above the Curie temperature the fracture resistance anisotropy is reversed.

load used in the experiments performed on MPAs. In such case, the parameter χ resulted in 0.14 ± 0.01.[1]

3.2. Temperature effect on poled and non-poled PZTs

The effect of temperature on the fracture resistance of poled and non-poled PZT specimens is presented in Fig. 6. The fracture resistance calculated with Eq. (1) for the non-poled specimens does not depend on the testing temperatures (reaching a maximal difference of 3.5% between RT and 400 °C) and is isotropic, *i.e.* same crack length parallel and normal to the longitudinal axis. The reason is that non-poled specimens have randomly oriented domains (since they have not been poled before). Therefore temperature cannot undergo any depolarisation effect. On the other hand, for the poled specimens, fracture resistance anisotropy can be appreciated depending on the crack orientation (*i.e.* parallel or normal to the poling axis). The maximum and minimum fracture resistance values are reached at room temperature in direction parallel and normal to the poling axis respectively (resulting in $K_F^{//} = 1.51 \pm 0.02\,\text{MPa m}^{1/2}$ and $K_F^{\perp} = 0.62 \pm 0.01\,\text{MPa m}^{1/2}$). As the testing temperature increases, $K_F^{//}$ and $K_F^{\perp}$ vary slightly leading to smaller and higher fracture resistance values respectively, reaching a minimum and a maximum above the Curie temperature of $K_F^{//} = 0.99 \pm 0.02\,\text{MPa m}^{1/2}$ and $K_F^{\perp} = 1.00 \pm 0.02\,\text{MPa m}^{1/2}$ respectively.

The change in fracture resistance after exposure at different temperatures is associated with the domain switching process activated by the thermal loading. It can be inferred from Fig. 6 that from temperatures above 75 °C some of the domains (initially oriented parallel to the longitudinal/poling axis) may have recovered their original orientation (depolarisation effect), thus affecting the initial fracture resistance of the material. It can be also seen that the decrease in fracture resistance in the parallel direction is counterbalanced by an increase in the normal direction. Above the Curie temperature, the material is no longer polarised, and thus the fracture resistance measured after 400 °C is almost equal to that of a non-poled (isotropic) material, *i.e.* $K_F = 1.09 \pm 0.02\,\text{MPa m}^{1/2}$.

3.3. Combined thermo-mechanical effect on poled PZTs

The effect of mechanical loading (compression along the longitudinal axis) combined with the temperature effect on the fracture resistance of poled PZT specimens is presented in Figs. 7 and 8 for a mechanical stresses of $\sigma = -25$ MPa and $\sigma = -50$ MPa respectively.

The fracture resistance measured in poled PZT specimens after being mechanically stressed at $\sigma = -25$ MPa (compression) at elevated temperatures shows a slightly change in K_F for testing temperatures between 25 °C and 150 °C (Fig. 7). However,

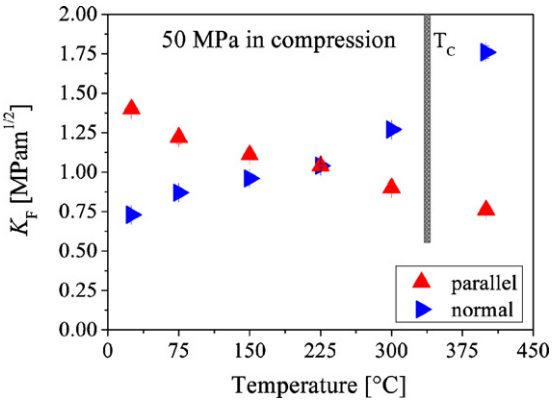

Fig. 8. Fracture resistance measured in poled PZT specimens after being mechanically stressed at $\sigma = -50$ MPa (compression) at elevated temperatures. The mechanical stress applied against the direction of poling yields a significant depolarisation effect even at low temperatures. The fracture resistance anisotropy of the PZT reverses for temperatures above 225 °C, reaching values up to 1.75 MPa m$^{1/2}$ for 400 °C.

[1] The indentation load was selected as low as 1.96 N to reduce the effect of the nearby electrodes, but high enough to get cracks out of the indentation imprint.

a significant change can be clearly seen for higher temperatures. For instance, at temperatures around 300 °C, the fracture resistance values in parallel and normal directions, *i.e.* $K_F^{//} = 1.04 \pm 0.02\,\mathrm{MPa\,m^{1/2}}$ and $K_F^{\perp} = 0.99 \pm 0.03\,\mathrm{MPa\,m^{1/2}}$ respectively, are practically the same as that of non-poled specimens (Fig. 6). The material has almost been brought to a state similar to the "as-sintered" state. Another interesting effect, which can be inferred from Fig. 7, is that for temperatures above the Curie point (*e.g.* 400 °C), the applied compressive stress along with the high temperature lead to a kind of mechanical polarisation in direction normal to the longitudinal axis, yielding opposite fracture resistance anisotropy (as compared with the initial poling state) in the material.

For the case of poled PZT specimens where a higher mechanical stress (compression), *i.e.* $\sigma = -50$ MPa, was applied along the direction of poling, an even more significant depolarisation effect was observed after lower exposure temperatures (Fig. 8). Likewise the previous case, the fracture resistance in parallel and normal directions, at temperatures *ca.* 225 °C, *i.e.* $K_F^{//} = 1.04 \pm 0.02\,\mathrm{MPa\,m^{1/2}}$ and $K_F^{\perp} = 1.04 \pm 0.01\,\mathrm{MPa\,m^{1/2}}$ respectively, coincide with the values for the non-poled specimens (Fig. 6); the material has been depolarised. From this temperature on (e.g. >225 °C) and due to the relatively high applied compressive stress ($\sigma = -50$ MPa), the fracture resistance anisotropy reverses, yielding higher fracture resistance in the direction normal to the longitudinal axis (Fig. 8). This phenomenon can be already observed below the Curie temperature. Finally, for temperatures beyond the Curie point (*e.g.* 400 °C), the fracture resistance normal to the longitudinal direction can reach values up to $K_F^{\perp} = 1.75\,\mathrm{MPa\,m^{1/2}}$, that is, even higher than $K_F^{//}$ at room temperature (corresponding to a hypothetical "fully" poled PZT material). This finding indicates that the alignment of domains along the poling axis provided by the application of an electrical field above the coercive field strength of the material does not lead to a fully polarised state of the PZT material, as it has been stated by other authors.[25] However, the use of the ferroelastic effect, *i.e.* domain switching in direction normal to the applied mechanical stress, may lead to a maximum of domain orientation, and thus a significant increase in the fracture resistance potential of the PZT material. Nevertheless, as commented above, the increase in fracture resistance normal to the longitudinal axis is counterbalanced by a decrease in the parallel direction. In other words, the shielding effect associated with the increase amount of domains oriented in the normal direction (in case of MPAs parallel to the electrodes) will yield a corresponding decrease of the fracture resistance in the other direction, *i.e.* perpendicular to the electrodes. This effect may be of importance in the case of multilayered actuators, where the propagation of cracks from outer terminal electrode through the whole stack to the other outer electrode (*i.e.* parallel to the poling direction) may cause the failure of the actuator.

3.4. Depolarisation effects through mechanical compression in MPAs

A typical indentation imprint performed in both the active and passive regions of a poled stack and the corresponding cracks emerging from the edges of the imprint can be seen in Fig. 9. The roughness developed around the indent is associated with the ferroelastic effect (domain switching due to mechanical stress) around the imprint, caused by the indentation stress field. This may be experimental evidence of the relaxation effects due to ferroelastic domain switching around an indentation.[26,27]

The total crack length ($2c$) was measured in both horizontal and vertical directions in the active and passive regions of the stacks. Fig. 10 shows the corresponding fracture resistance in both regions determined with Eq. (1) as a function of the compressive mechanical load applied to the poled MPAs.

A clear difference between normal and parallel fracture resistance can be appreciated in both the active (Fig. 10a) and the passive (Fig. 10b) zones of the MPA. After poling the stack, the domains in the active zone are oriented along the longitudinal axis (parallel direction), *i.e.* axis of the application of the electrical field. When an indentation is performed in this zone, the

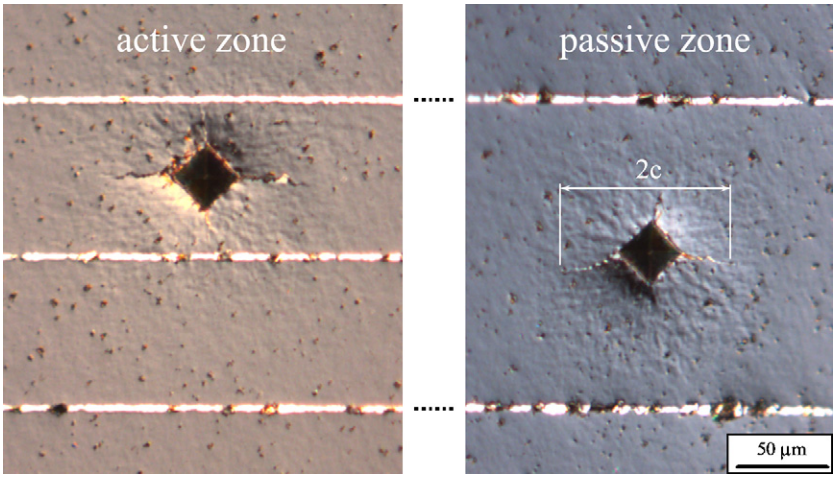

Fig. 9. Optical micrographs using Nomarski interference to show indentation imprints in the active (left) and passive (right) zone of a poled stack. The roughness developed around the indent is associated with the ferroelastic effect (domain switching due to mechanical stress) in the indentation zone. The total crack length ($2c$) is measured in both horizontal and vertical directions.

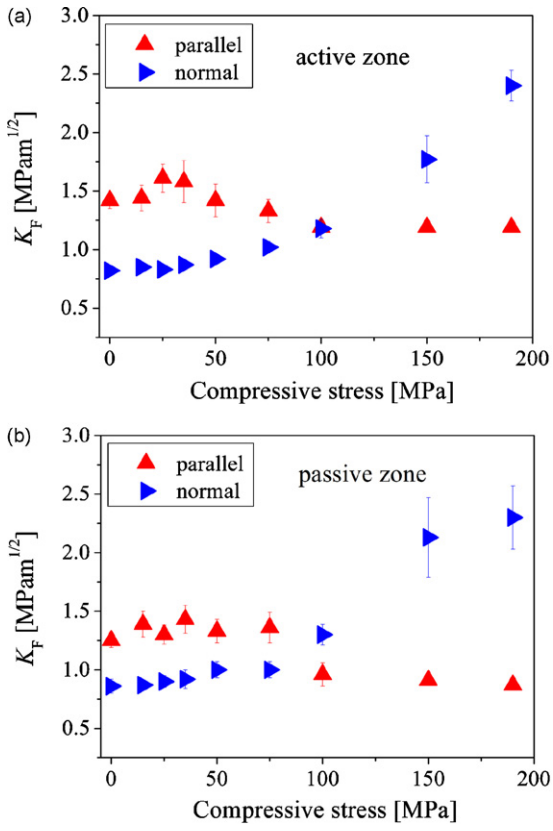

Fig. 10. Fracture resistance measured in the (a) active and (b) passive regions of MPA specimens after applying different mechanical (compressive) stresses. The depolarisation process due to the mechanical loading shows the ferroelastic behaviour in the actuator. The fracture resistance increases with the mechanical stress normal to the poling direction due to reorientation of domains.

stresses at the crack tip (normal to the crack wake) may switch the domains (90° switching) that are oriented normal to it.[11] In the case of normal cracks, the stress at the tip has the same direction as the domains (longitudinal axis), and thus no switching effects can be observed. For that reason normal cracks can extend further and, as a consequence, $K_F^{\perp}$ is lower (Fig. 10a). On the other hand, the stress at the tip of the parallel cracks is perpendicular to the domain orientation, and thus, some of the domains may switch due to the ferroelastic effect. This process implies an energy consumption, which acts as a fracture resistance mechanism (shielding) in the piezo-ceramic: $K_F^{//}$ is higher.[2] This effect can be clearly seen in poled stacks without pre-compression, *i.e.* at $\sigma = 0$ MPa in Fig. 10a.

An analogous result is found in the passive region, *i.e.* fracture resistance is different in normal and parallel directions. During the poling process a piezoelectric strain in the active region causes (ferro-)elastic strain in the passive zone. Hence, fracture resistance anisotropy can be observed even in the passive region (Fig. 10b).

[2] We caution the reader that the fracture resistance in parallel direction evaluated in poled MPAs, *i.e.* in direction perpendicular to the electrodes, is influenced by the position of such electrodes, and thus, the $K_F^{//}$ values presented should be taken with care.

The effect of mechanical loading on the fracture resistance of poled stacks, in both active and passive regions, has been evaluated by applying a compressive load to the stack along its longitudinal direction (poling axis). This way, and due to the ferroelastic effect, some of the domains oriented longitudinally due to the poling process are prone to switch (depolarisation process). This switching yields a different crack resistance in normal and parallel directions as for the case of PZT bulk material.

It can be inferred from Fig. 10 that the effect of compressive loading on the fracture resistance cannot be clearly observed below $\sigma = -50$ MPa. The fact that no significant differences in crack length below $\sigma = -50$ MPa are discerned is associated with the small proportion of domains that switch under such mechanical conditions. It is worthy to point out that the typical pre-stress level applied to actuators of this kind (*ca.* $\sigma = -25$ MPa) therefore has no significant effects on the fracture resistance at room temperature, as inferred from Fig. 10. However, in an attempt to see some depolarisation effects on the fracture resistance, applied loads were increased up to -190 MPa. As a result, for compression loads higher than -50 MPa fracture resistance anisotropy could be seen between $\sigma = -50$ MPa and $\sigma = -190$ MPa (Fig. 10). It can be observed that a plateau region of fracture resistance normal to the poling direction is reached in the passive region of the actuator (Fig. 10b), whereas in the active region (Fig. 10a) an increase trend in fracture resistance can be still appreciated. This suggests that a small reservoir of switchable domains may be still available. Regarding the fracture resistance parallel to the poling direction, a constant value is achieved in both passive and active regions owed to the constraining effect of the electrodes to the crack growth.

As commented in Section 3.3, the fracture resistance anisotropy in MPAs may be of extreme importance since the propagation of cracks from electrode to electrode (*i.e.* parallel to the poling direction) can cause the failure of the stack functionality. An important result of this study performed on bulk PZTs and then extended to MPAs is that the combination of mechanical loads and temperature should be taken into account when the maintenance of the structural and functional integrity of piezoelectric multilayer actuators in terms of crack propagation is pursued. Although it has been demonstrated that the only effect of temperature does not lead to a significant depolarisation effect on bulk PZTs, future studies should be performed on MPAs combining the effect of mechanical stress and temperature for fracture resistance evaluation.

4. Concluding remarks

The fracture resistance of a commercial soft PZT material as a function of temperature and mechanical stress on electrically poled specimens has been evaluated using the indentation fracture (IF) method. The fracture resistance reached at room temperature in direction parallel and normal to the poling axis resulted in $K_F^{//} = 1.51 \pm 0.02$ MPa m$^{1/2}$ and $K_F^{\perp} = 0.62 \pm 0.01$ MPa m$^{1/2}$, respectively, as compared with that of a non-poled (isotropic) specimen, $K_F = 1.09 \pm 0.02$ MPa m$^{1/2}$, taken as a reference. The increase in temperature leads to a light,

gradually depolarisation of the material, until the Curie temperature is reached and the material is full depolarised. The additional mechanical compressive stress enhances such depolarisation effect with the temperature, leading to a full depolarised material even below the Curie point. This depolarisation effects yield a change in the fracture resistance of the material in direction normal and parallel to the poling direction, which will influence the crack propagation direction. In this regard, a PZT-based multilayered piezoelectric actuator (MPA) has been additionally investigated as a function of the pre-stressed conditions. Experiments show a clear anisotropy (parallel or perpendicular to the poling direction) in the resistance to crack propagation of the piezo-ceramic. Although no significant effects in the fracture resistance can be observed for typical pre-stress levels applied to actuators of this kind (*ca.* $\sigma = -25$ MPa), a decrease of the fracture resistance in direction perpendicular to the electrodes occurs for higher compression loads. This effect is important in the case of MPAs, where the propagation of cracks from outer terminal electrode through the whole stack to the other outer electrode may cause a failure of the actuator and therefore should be taken into account in the MPA design.

Acknowledgements

Financial support by the Österreichische Forschungsförderungsgesellschaft mbH, the Province of Styria, the Steirische Wirtschaftsförderungsgesellschaft GmbH and the Municipality of Leoben within research activities of the Materials Center Leoben under the frame of the Austrian Kplus Competence Center Programme is gratefully acknowledged. The authors express their gratitude to Mr. Franz Aldrian and Mr. Wolfgang Athenstaedt (EPCOS OHG, Deutschlansberg, Austria) for their assistance with specimen preparation.

References

1. Uchino, K., Piezoelectric actuators and ultrasonic motors. In *Electronic Materials: Science and Technology*, ed. H. L. Tuller. Kluwer Academic Publishers, 1997.
2. Setter, N., *Piezoelectric Materials in Devices, Ceramics Laboratory, EPFL*. Swiss Federal Institute of Technology, 2002.
3. Pritchard, J., Bowen, C. R. and Lowrie, F., Multilayer actuators: review. *Br. Ceram. Trans.*, 2001.
4. Cao, H. and Evans, A. G., Non linear deformation of ferroelectric ceramics. *J. Am. Ceram. Soc.*, 1993, **76**, 890–896.
5. Supancic, P., Wang, Z., Harrer, W., Reichmann, K. and Danzer, D., Strength and fractography of piezoceramic multilayer stacks. *Key Eng. Mat.*, 2005, **290**, 46–53.
6. Kuna, M. Fracture mechanics of piezoelectric materials—where are we right now? Eng. Fract. Mech., in press, doi:10.1016/j.engfracmech.2009.03.016.
7. Furata, A. and Uchino, K., Dynamic observation of crack propagation in piezoelectric multilayer actuators. *J. Am. Ceram. Soc.*, 1993, **76**, 1615–1617.
8. Schneider, G. A., Influence of electric field and mechanical stresses on the fracture of ferroelectrics. *Annu. Rev. Mater. Res.*, 2007, **37**, 491–538.
9. Okasaki, K., Mechanical behavior of ferroelectric ceramics. *Ceram. Bull.*, 1984, **63**(9), 1150–1157.
10. Lynch, C., Fracture of ferroelectric and relyor ceramics: influence of electric field. *Acta Mater.*, 1998, **46**(2), 599–608.
11. Schneider, G. A. and Heyer, V., Influence of the electric field on Vickers indentation crack growth in $BaTiO_3$. *J. Eur. Ceram. Soc.*, 1999, **19**, 1299–1306.
12. Kolleck, A., Schneider, G. A. and Meschke, F., R-curve behaviour of $BaTiO_3$ and PZT ceramics under the influence of an electric field applied parallel to the crack front. *Acta Mater.*, 2000, **48**, 4099–4113.
13. Fett, T., Glazounov, A., Hoffmann, M. J., Munz, D. and Thun, G., On the interpretation of different R-curves for soft PZT. *Eng. Fract. Mech.*, 2001, **68**, 1207–1218.
14. Meschke, F., Raddatz, O., Kolleck, A. and Schneider, G. A., R-curve behavior and crack-closure stresses in barium titanate and (Mg, Y)-PSZ ceramics. *J. Am. Ceram. Soc.*, 2000, **83**(2), 353–361.
15. Lucato, S., Lupascu, D. and Rödel, J., Effect of poling direction on R-curve behavior in lead zirconate titanate. *J. Am. Ceram. Soc.*, 2000, **83**(2), 424–426.
16. Fett, T., Munz, D. and Thun, G., Bending strength of a PZT ceramic under electric fields. *J. Eur. Ceram. Soc.*, 2003, **23**, 195–202.
17. Kounga Njiwa, A. B., Fett, T., Lupascu, D. C. and Rödel, J., Effect of geometry and electrical boundary conditions on R-curves for lead zirconate titanate ceramics. *Eng. Fract. Mech.*, 2006, **73**(3), 309–317.
18. Lupascu, D. C., Genenko, Y. A. and Balke, N., Aging in ferroelectrics. *J. Am. Ceram. Soc.*, 2006, **89**(1), 224–229.
19. Kreith, J., Grünbichler, H. and Bermejo, R. Adaptation of a materials testing machine to characterise multilayer piezoelectric actuators. J. Electroceram., submitted for publication.
20. Anstis, G. R., Chantikul, P. and Lawn, B. R., A critical evaluation of indentation techniques for measuring fracture toughness: I. Direct crack measurements. *J. Am. Ceram. Soc.*, 1981, **64**, 533–538.
21. Kübler, J. Procedure for determining the fracture toughness of ceramics using the single-edge-V-notched beam (SEVNB) method, Bericht für EMPA, Swiss Federal Laboratories for Materials Testing and Research.
22. Damani, R., Gstrein, R. and Danzer, R., Critical notch-root radius effect in SENB-S fracture toughness testing. *J. Eur. Ceram. Soc.*, 1996, **16**, 695–702.
23. ENV-843-1, *Advanced Technical Ceramics, Monolithic Ceramics, Mechanical Properties at Room Temperature, Part 1: Determination of flexural Strength*., 1995.
24. Srawley, J. E., Wide range stress intensity factor expressions for ASTM E399 standard fracture toughness specimens. *Int. J. Fract.*, 1976, **12**, 475–476.
25. Hall, A., Allahverdi, M., Akdogan, E. and Safari, A., Development and electromechanical properties of multimaterial piezoelectric and electrostrictive PMN-PT monomorph actuators. *J. Electroceram.*, 2005, **15**(2), 143–150.
26. Hall, D. A., Steuwer, A., Cherdhirunkorn, B., Withers, P. J. and Mori, T., Texture of poled tetragonal PZT detected by synchrotron X-ray diffraction and micromechanics analysis. *Mater. Sci. Eng. A*, 2005, **409**(1–2), 206–210.
27. Kungl, H., Theissmann, R., Knapp, M., Baehtz, C., Fuess, H., Wagner, S., Fett, T. and Hoffmann, M. J., Estimation of strain from piezoelectric effect and domain switching in morphotropic PZT by combined analysis of macroscopic strain measurements and synchrotron X-ray data. *Acta Mater.*, 2007, **55**(6), 1849–1861.